Indian Geotechnical Journal, 32 (4), 2002

Active Thrust on Bracing System of Open Cuts in Cohesion-less Soil - Point of Application

D.M. Dewaikar* and S.A. Halkude†

Introduction

The deformation of a braced wall differs from the deformation condition of a retaining wall, in that, in a braced wall, the rotation is about the top. For this reason, neither Coulomb's nor Rankine's theory will give the actual earth pressure distribution. This fact is illustrated in Fig.1, in which, AB is a wall retaining cohesion-less backfill. When the wall deforms to the position AB′, failure surface BC develops. Since the upper portion of the soil mass in the zone ABC does not undergo sufficient deformation, it does not pass into active state. The sliding surface BC intersects the ground surface at 90° (Terzaghi, 1943). The corresponding earth pressure distribution on the wall will not be linearly varying, but somewhat parabolic as shown in Fig.1. With this type of pressure distribution, the point of application of the resultant active thrust, P_a will be at a height of n_aH, measured from the wall base, with $n_a > 1/3$. Theoretical considerations and field measurements have shown that, n_a could be as high as 0.55 (Terzaghi, 1943).

The theoretical estimation of the active thrust on the bracing system of open cuts can be done by method of trial wedges (Terzaghi, 1943) and using this method, Kim and Preber (1969) have reported the values of active earth pressure coefficient, K_a, for various ranges of angles of soil internal friction, ϕ, wall friction, δ and n_a.

In the trial wedge method of analysis, an assumption is required

* Corresponding Author. Professor in Civil Engineering Department, Indian Institute of Technology, Bombay, Mumbai-400 076, India Tel.: 91-22-5767325; Fax No.91-22-5767302. E-mail: dmde@civil.iitb.ernet.in

† Research Scholar in Civil Engineering Department, Indian Institute of Technology, Bombay, Mumbai- 400 076, India

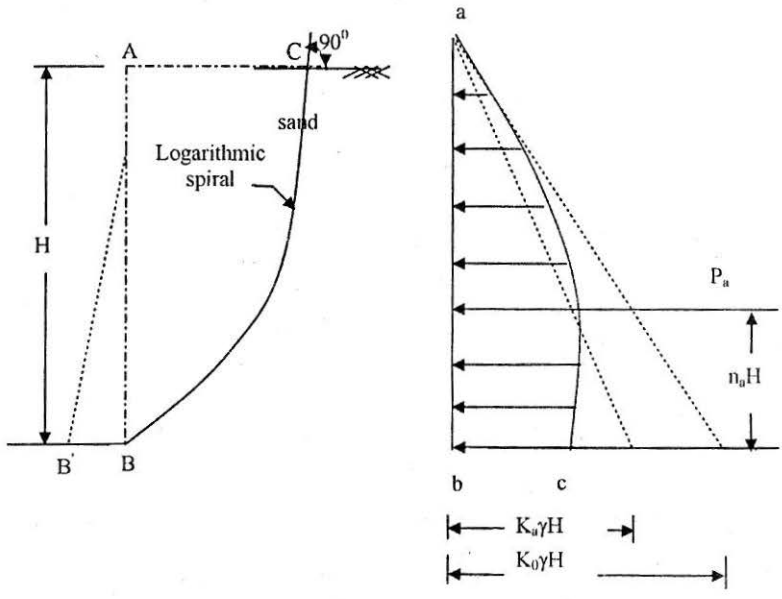

FIGURE 1 : Earth Pressure Distribution against a Wall with Rotation about Top

regarding the location of point of application of active thrust, P_a so as to make it statically determinate. The solution that is obtained is therefore, not unique.

With this observation, a method of the analysis is proposed in this paper for the evaluation of active thrust and its point of application, based on the application of Kötter's (1903) equation. The details of this method are as described below.

Geometry of the Problem

In Fig.2, MBK represents the profile of a vertical cut in cohesion-less soil and BG represents a (log spiral) failure surface. At point, G, the tangent, EG to the log spiral makes an angle of 90° with the horizontal and the radial line, QA of the log spiral makes an angle, ϕ with the horizontal.

At point, B at the wall base, the tangent, RS to the log spiral makes an angle, θ_L with the horizontal and line, TV is normal to the tangent, RS. D is any point on the log spiral, corresponding to the angle, θ as measured from the radial line, QGA and tangent to the log spiral at D, makes an angle α with the horizontal. θ_m represents the polar angle corresponding to the point, B and line, ZBA which makes an angle, ϕ with the normal, TV

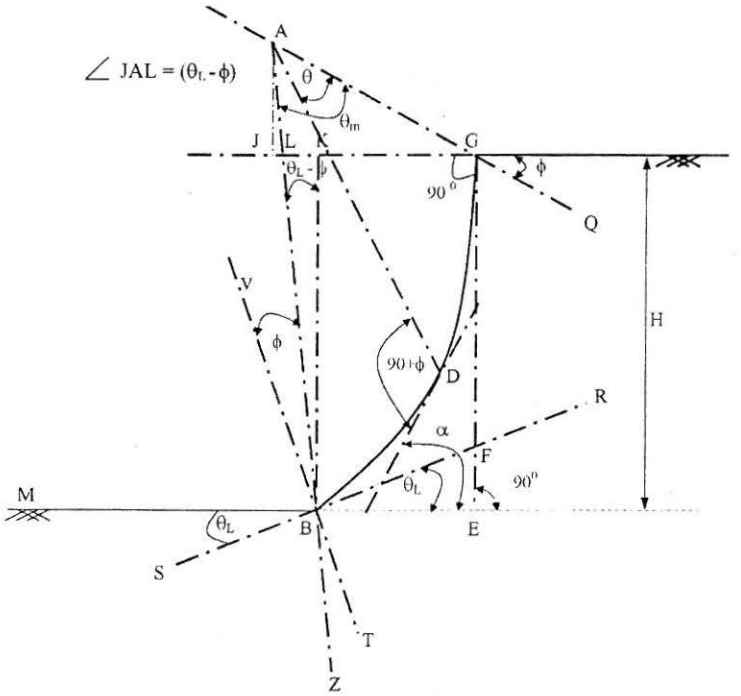

FIGURE 2 : Geometry of the Problem

at B, is another radial line of the log spiral. Its point of intersection, A with the radial line, QA is the pole of the log spiral.

From the above-referred figure, the following relationships are obtained,

$$\theta_L + \theta_m = 90 \tag{1a}$$

and $$\alpha = 90 - \theta \tag{1b}$$

If the height, BK of the cut is designated as H, then, following useful expressions are further obtained from the geometry of Fig.2.

$$LB = H/\cos(\theta_L - \phi) \tag{2a}$$

$$AB = AG\, e^{\theta_m \tan\phi} \tag{2b}$$

and $$AB = AL + LB$$

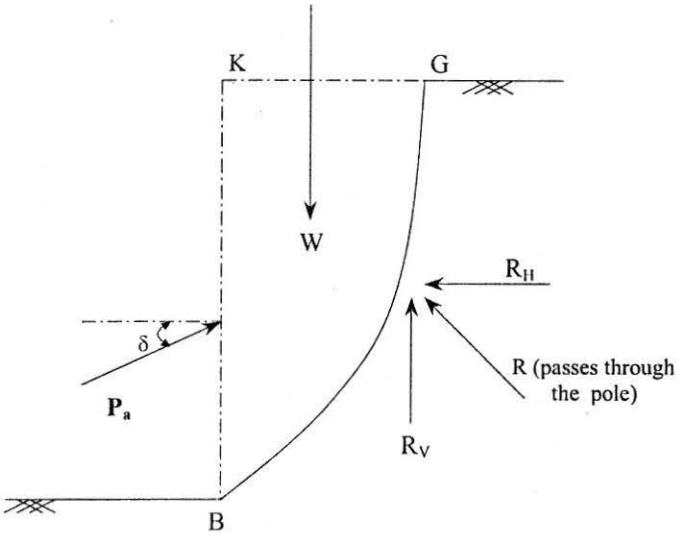

FIGURE 3 : Free Body Diagram of Failure Wedge BKG

The distance AL is given as,

$$AL = \frac{LB\sin\phi}{\left[\cos(\theta_L - \phi)e^{\theta_m \tan\phi} - \sin\phi\right]} \qquad (2c)$$

Thus, with the distance, AB being known, initial radius, AG (or r_o) of the log spiral can be determined.

From the above relationships, entire geometry, specific to this problem, can be described for a specified H, in terms of angle, θ_L. By changing θ_L, different failure surfaces, consistent with the geometry of the problem, are generated.

Outline of the Method of Analysis

In Fig.3, free body diagram of trial failure wedge, BKG is shown. The forces that act on this wedge are,

1. weight of the wedge, W

2. active thrust, P_a, inclined at an angle, δ to the normal to the wall

3. horizontal component, R_H and vertical component, R_V of the resultant reaction, R that acts on the failure surface, BG. These components are determined using Kötter's equation, and therefore, these are known forces.

The only unknown force among the above-described forces is P_a. Now, if the trial value of θ_L is correctly predicted, the values of P_a that are obtained from two force equilibrium conditions will be the same, otherwise they will be different. If they are different, another trial failure surface is generated by changing the value of θ_L and again the forces W, R_H, and R_V are computed. These trials are continued till the two values of P_a converge to the specified (four) decimal accuracy.

After satisfying force equilibrium conditions, the moment equilibrium condition is used to obtain the location of the point of application of P_a, by taking moments of the forces about pole, A of the log spiral.

Computation of Components of Resultant Reaction on the Curved Failure Surface

For this purpose as mentioned earlier, Kötter's equation for active state in cohesion-less soil medium is integrated over the curved failure surface, BG. The equation is available in the following form,

$$\frac{dp}{ds} - 2p\tan\phi\frac{d\alpha}{ds} = \gamma\sin(\alpha-\phi) \tag{3}$$

where

p = magnitude of distributed soil reaction at a point (such as D in Fig.2), with direction along the radial line at D.

ds = elemental length of failure surface (at D)

α = inclination of tangent to the failure surface at a point (D)

ϕ = angle of soil internal friction and

γ = soil unit weight

The integration of above equation with the condition that pressure at point G (Fig.2) is zero, yields the following solution,

$$p = \frac{\gamma r_o \sec\phi}{\left(1+9\tan^2\phi\right)}\left[p_1 + p_2 + p_3\right] \tag{4a}$$

where

$$p_1 = 3\tan\phi\cos(\theta+\phi)e^{\theta\tan\phi} \tag{4b}$$

$$p_2 = \sin(\theta+\phi)e^{\theta\tan\phi} \tag{4c}$$

$$p_3 = -4\sin\phi e^{-2\theta\tan\phi} \tag{4d}$$

With the evaluation of distribution of reaction on the curved failure surface, the horizontal and vertical components of resultant reaction can be computed.

Computation of horizontal component

For the elemental length, ds at point, D (Fig.2), the elemental force, dR is given as,

$$dR = p\,ds \tag{5}$$

The component dR_H, of this force in the horizontal direction is given as,

$$dR_H = p\,ds\cos(\theta+\phi) \tag{6}$$

Therefore, the component, R_H will be given as,

$$R_H = \int_0^{\theta_m} p\cos(\theta+\phi)ds \tag{7}$$

In the above equation, ds can be expressed as,

$$ds = r\,d\theta\sec\phi \tag{8}$$

where r = radial distance of the point (such as D) with the corresponding polar angle θ.

Substitution of p from Eqn.4a and ds from Eqn.8 can be made in Eqn.7 and integration can be performed with the limits of θ from 0 to θ_m to obtain the following result.

$$R_H = \frac{\gamma r_o^2\sec^2\phi}{2(1+9\tan^2\phi)}\left[R_{H1}+R_{H2}+R_{H3}-R_{H4}\right] \tag{9a}$$

The parameters in the bracket are as given below.

$$R_{H1} = 1.5\left[e^{2\theta_m\tan\phi}-1\right] \tag{9b}$$

$$R_{H2} = \left[\frac{3\tan\phi}{4\sec^2\phi}\right]\left[R_1 + R_2 + R_3\right] \tag{9c}$$

where $R_1 = 2\tan\phi\cos\left(2\theta_m + 2\phi\right)e^{2\theta_m\tan\phi}$

$R_2 = 2\sin\left(2\theta_m + 2\phi\right)e^{2\theta_m\tan\phi}$

and $R_3 = -2\tan\phi\cos 2\phi - 2\sin 2\phi$

$$R_{H3} = \frac{\cos^2\phi}{4}\left[R_4 + R_5 + R_6\right] \tag{9d}$$

where $R_4 = 2\tan\phi\sin\left(2\theta_m + 2\phi\right)e^{2\theta_m\tan\phi}$

$R_5 = -2\cos\left(2\theta_m + 2\phi\right)e^{2\theta_m\tan\phi}$

and $R_6 = -2\tan\phi\sin 2\phi + 2\cos 2\phi$

$$R_{H4} = \left[\frac{8\sin\phi}{\sec^2\phi}\right]\left[R_7 + R_8\right] \tag{9e}$$

where $R_7 = -\tan\phi\cos\left(\theta_m + \phi\right)e^{-\theta_m\tan\phi}$ and

$R_8 = \sin\left(\theta_m + \phi\right)e^{-\theta_m\tan\phi}$

Computation of Vertical Component

The vertical component, dR_V of dR at point, D (Fig.2) is given as,

$$dR_V = p\,ds\sin\left(\theta + \phi\right) \tag{10}$$

The component, R_V will therefore be obtained as,

$$R_V = \int_0^{\theta_m} p\sin\left(\theta + \phi\right)ds \tag{11}$$

In the above expression, substitution for ds from Eqn.8 and p from Eqn.4a can be made and integration carried out to yield the following results:

$$R_V = \frac{\gamma r_o^2 \sec^2\phi}{2\left(1+9\tan^2\phi\right)}\left[R_{V1}+R_{V2}-R_{V3}-R_{V4}\right] \tag{12a}$$

The parameters in the bracket are as given below.

$$R_{V1} = \left[\frac{3\tan\phi}{4\sec^2\phi}\right]\left[R_9+R_{10}+R_{11}\right] \tag{12b}$$

where $R_9 = 2\tan\phi\sin\left(2\theta_m+2\phi\right)e^{2\theta_m\tan\phi}$

$R_{10} = -2\cos\left(2\theta_m+2\phi\right)e^{2\theta_m\tan\phi}$

and $R_{11} = -2\tan\phi\sin 2\phi+2\cos 2\phi$

$$R_{V2} = \left[\frac{1}{2\tan\phi}\right]\left[e^{2\theta_m\tan\phi}-1\right] \tag{12c}$$

$$R_{V3} = \left[\frac{1}{4\sec^2\phi}\right]\left[R_{12}+R_{13}+R_{14}\right] \tag{12d}$$

where $R_{12} = 2\tan\phi\cos\left(2\theta_m+2\phi\right)e^{2\theta_m\tan\phi}$

$R_{13} = 2\sin\left(2\theta_m+2\phi\right)e^{-2\theta_m\tan\phi}$ and

$R_{14} = -2\tan\phi\cos 2\phi-2\sin 2\phi$

Computation of Point of Application of Active Thrust

For this purpose, the moments of various forces about the pole of the log spiral are computed by referring to Fig.4.

Moment of Active Thrust about the Pole

The point of application of P_a is located at a distance n_aH from the wall base and at a distance, HX from the pole of log spiral. Therefore, the moment, M_1 of P_a about the pole, A is given as,

$$M_1 = HX\,P_a\cos\delta+JK\,P_a\sin\delta \tag{13}$$

in which, the distance, JK is given as,

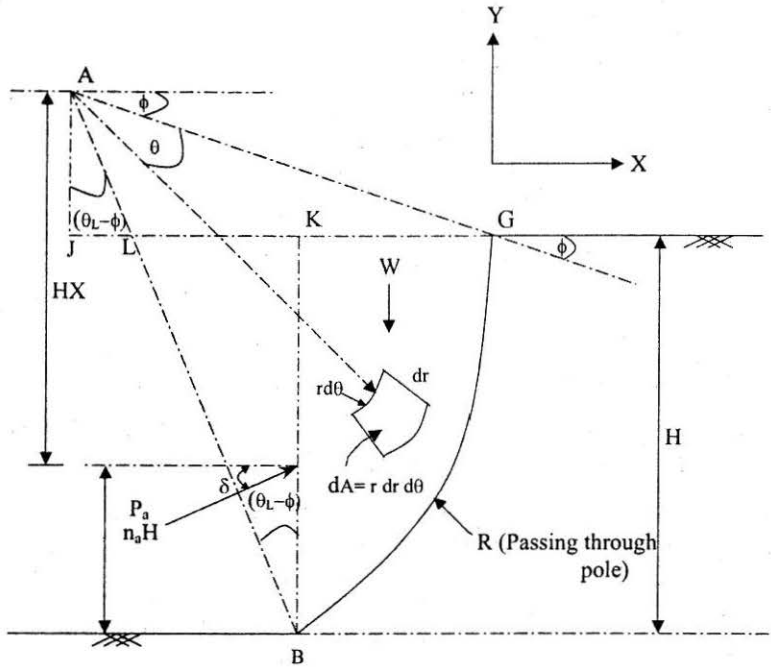

FIGURE 4 : Moment Calculations

$$JK = JL + LK$$
$$= r_o \sin\phi \tan(\theta_L - \phi) + H \tan(\theta_L - \phi) \quad (14)$$

Substituting the value of JK from Eqn.14 into Eqn.13, the moment, M_1 is obtained as,

$$M_1 = P_a \left[HX \cos\delta + \left\{ r_o \sin\phi \tan(\theta_L - \phi) + H \tan(\theta_L - \phi) \sin\delta \right\} \right] \quad (15)$$

Moment of Weight of Failure Wedge

The elemental area dA is given as,

$$dA = r\, dr\, d\theta \quad (16)$$

The weight, dW of this element is given as,

$$dW = \gamma\, r\, dr\, d\theta \quad (17)$$

The moment, dM_3, of dW about the pole is given as,

$$dM_3 = \gamma\, r\, dr\, d\theta\, r\cos(\theta+\phi) \tag{18}$$

and the moment of weight of entire segment, ABG, is given as,

$$M_3 = \int_0^{\theta_m}\int_0^{r} r^2 dr\, d\theta \cos(\theta+\phi)$$

or $$M_3 = \int_0^{\theta_m} \frac{r^3}{3}\cos(\theta+\phi)\,d\theta \tag{19}$$

Now, from the equation of log spiral, r is given as,

$$r = r_o e^{\theta\tan\phi}$$

Substituting for r in Eqn.19, the following result is obtained.

$$M_3 = \int_0^{\theta_m} \frac{r_o^3}{3}\cos(\theta+\phi)e^{3\theta_m\tan\phi}\,d\theta$$

or $$M_3 = \frac{r_o^3}{3}\int_0^{\theta_m} \cos(\theta+\phi)e^{3\theta_m\tan\phi}\,d\theta \tag{20}$$

Integration yields,

$$M_3 = \frac{\gamma\, r_o^3}{3\left(1+9\tan^2\phi\right)}\left[M_{22}+M_{23}+M_{24}\right] \tag{21a}$$

where $$M_{22} = 3\tan\phi\cos(\theta_m+\phi)e^{3\theta_m\tan\phi} \tag{21b}$$

$$M_{23} = \sin(\theta_m+\phi)e^{3\theta_m\tan\phi} \tag{21c}$$

and $$M_{24} = -4\sin\phi \tag{21d}$$

From the above moment, deductions are made, which correspond to the moment, M_{25} of the weight of the triangular area, ALG about the pole and moment, M_{26} of weight of triangular area BLK, about the pole as shown in the Fig.4. These moments are computed as,

$$M_{25} = \frac{1}{6}\gamma r_o^3 \cos^2\phi \sin\phi - \frac{1}{6}\gamma r_o^3 \sin^3\phi \tan^2(\theta_L - \phi) \quad (22a)$$

and $$M_{26} = \gamma H^2 \tan(\theta_L - \phi)\left\{r_o \sin\phi \tan(\theta_L - \phi) + \frac{2}{3} H \tan(\theta_L - \phi)\right\}$$

or $$M_{26} = \gamma H^2 \tan^2(\theta_L - \phi)\left\{r_o \sin\phi + \frac{2}{3} H\right\} \quad (22b)$$

Thus, the moment M_2, of self-weight of the failure soil wedge about the pole of log spiral is finally given as,

$$M_2 = M_3 - M_{25} - M_{26} \quad (23)$$

By equating the expressions as given by Eqn.15 and Eqn.23, HX can be computed by referring to Fig.4, the distance, $n_a H$ will be given as,

$$n_a H = H - HX + r_o \sin\phi \quad (24)$$

Results and discussion

The active thrust that is obtained from the above computations is expressed in a non-dimensional form, as its ratio with respect to $\frac{1}{2}\gamma H^2$, which gives the magnitude of active earth pressure coefficient, K_a.

The values of K_a and n_a have been computed for several combinations of ϕ and δ and in Table 1, the results are reported along with those of Kim and Preber (1969).

The influence of angle of soil internal friction on K_a can be clearly seen from the proposed values. For example for δ = 5°, K_a decreases from 0.580 for ϕ = 15° to 0.189 for ϕ = 45° and similar trend is shown by the data reported by Kim and Preber.

As compared to ϕ, the influence of δ on K_a appears to be lesser degree. For example, for ϕ = 45°, K_a varies from 0.182 to 0.193 with increasing from 0 to 45° and for ϕ = 25°, K_a varies from 0.425 to 0.337, with increasing from 0 to 25°. The data reported by Kim and Preber also shows the similar trend.

The location of point of application as obtained from the proposed analysis is found to be not very sensitive to the changes in ϕ or δ values. For example, for ϕ = 35°, n_a varies from 0.486 to 0.448, with δ increasing

TABLE 1 : Values of $P_a/0.5\gamma H^2$

ϕ (deg)	δ (deg)	η = 0.3	η = 0.4	η = 0.5	η = 0.6	Proposed Values	
						$P_a/0.5\gamma H^2$	η
	0	0.542	0.602	0.679	0.778	0.609	0.409
	5	0.518	0.575	0.646	0.739	0.58	0.408
15	10	0.505	0.559	0.629	0.719	0.561	0.402
	15	0.499	0.554	0.623	0.714	0.549	0.393
	0	0.499	0.495	0.551	0.622	0.511	0.431
	5	0.43	0.473	0.526	0.593	0.488	0.43
20	10	0.419	0.46	0.511	0.575	0.472	0.426
	15	0.413	0.454	0.504	0.568	0.462	0.419
	20	0.413	0.454	0.504	0.569	0.457	0.409
	0	0.371	0.405	0.447	0.499	0.425	0.451
	5	0.356	0.389	0.428	0.477	0.407	0.45
25	10	0.347	0.378	0.416	0.464	0.395	0.447
	15	0.342	0.373	0.41	0.457	0.387	0.441
	20	0.341	0.372	0.409	0.456	0.383	0.434
	25	0.344	0.375	0.413	0.461	0.383	0.423
	0	0.304	0.33	0.361	0.4	0.351	0.47
	5	0.293	0.318	0.347	0.384	0.337	0.469
	10	0.286	0.31	0.339	0.374	0.328	0.466
30	15	0.282	0.306	0.334	0.368	0.322	0.461
	20	0.281	0.305	0.332	0.367	0.319	0.455
	25	0.284	0.307	0.335	0.37	0.319	0.447
	30	0.289	0.313	0.341	0.377	0.322	0.436
	0	0.247	0.267	0.29	0.318	0.286	0.486
	5	0.239	0.258	0.28	0.307	0.276	0.485
	10	0.234	0.252	0.273	0.3	0.269	0.483
	15	0.231	0.249	0.27	0.296	0.265	0.479
35	20	0.231	0.248	0.269	0.295	0.263	0.474
	25	0.232	0.25	0.271	0.297	0.263	0.467
	30	0.236	0.254	0.276	0.302	0.266	0.459
	35	0.243	0.262	0.284	0.312	0.272	0.448

TABLE 1 : Continued .....

ϕ (deg)	δ (deg)	η = 0.3	η = 0.4	η = 0.5	η = 0.6	Proposed Values	
						$P_a/0.5\gamma H^2$	η
	0	0.198	0.213	0.23	0.252	0.23	0.501
	5	0.192	0.206	0.223	0.244	0.24	0.598
	10	0.189	0.202	0.219	0.238	0.218	0.498
	15	0.187	0.2	0.216	0.236	0.215	0.495
40	20	0.187	0.2	0.216	0.235	0.214	0.491
	25	0.188	0.202	0.218	0.237	0.215	0.485
	30	0.192	0.205	0.222	0.241	0.217	0.478
	35	0.197	0.211	0.228	0.248	0.226	0.469
	40	0.205	0.22	0.237	0.259	0.193	0.458
	0	0.156	0.167	0.18	0.196	0.182	0.514
	5	0.152	0.163	0.175	0.19	0.189	0.603
	10	0.15	0.16	0.172	0.187	0.174	0.512
	15	0.148	0.159	0.171	0.185	0.172	0.509
	20	0.149	0.159	0.171	0.185	0.171	0.506
45	25	0.15	0.16	0.173	0.187	0.172	0.501
	30	0.153	0.164	0.176	0.19	0.175	0.495
	35	0.158	0.168	0.181	0.196	0.179	0.488
	40	0.164	0.175	0.188	0.204	0.185	0.479
	45	0.173	0.184	0.198	0.213	0.193	0.467

from 0 to 35°. Similarly, for δ = 10°, n_a varies from 0.402 for ϕ = 15° to 0.512 for ϕ = 45°. From the table, it is also seen that, most of the n_a values are in the range of 0.45 to 0.50, whereas, a value of as high as 0.55 is reported on the basis of some theoretical considerations and field measurements (Terzaghi, 1943).

From Table 1, it is further seen that, proposed K_a values are quite close to those reported by Kim and Preber, if the corresponding n_a values are approximately equal. For example, for ϕ = 40° and δ = 0°, the proposed K_a and n_a values are 0.230 and 0.501 respectively and value of K_a corresponding to n_a = 0.5, from the data of Kim and Preber is 0.230. Similarly, for ϕ = 45° and δ = 0°, proposed K_a and n_a values are 0.189 and 0.603 respectively and from the data of Kim and Preber, corresponding to n_a = 0.6, the K_a value is 0.190.

It may be finally noted that, the values of K_a and n_a as obtained from the proposed analysis are the unique ones, since these are based on the compliance of force and moment equilibrium conditions. Kötter's equation lends itself as a powerful tool in the formulation of an analysis, in which no assumptions are required.

Conclusions

The main conclusions that emerge from this analysis are as follows:

1. A unique analysis of active thrust and its point of application is possible for open cuts in cohesion-less soil, using Kötter's equation.

2. The point of application of active thrust depends to a certain extent on angles of soil and wall friction.

3. To a large extent, the point of application is located around a distance of 0.45H to 0.50H from the wall base.

References

JUMIKIS, A.R. (1969) : *Theoretical Soil Mechanics*, Van Nostrand Reinhold Company, Canada.

KIM, J.S. and PREBER, T. (1969) : "Earth Pressure against Braced Excavations", *Journal of Soil Mechanics and Foundation Division*, ASCE, Vol.95, No.SM6, pp.1581-1584.

TERZAGHI, K. (1943) : *Theoretical Soil Mechanics*, John Wiley & Sons Inc., New York.